International Journal of Research in Advent Technology, Special Issue, August 2018
E-ISSN: 2321-9637
International Conference on "Topical Transcends in Science, Technology and Management" (ICTTSTM-2018)
Available online at www.ijrat.org

Solution Combustion Synthesis, Characterization and Photo Catalytic Activity of $Dy_{0.5}Zr_{0.5}O_{1.75}$ (Dysprosium Zirconium Oxide) Nanopowder

Rajeshwari G, Dr. Chandrappa G.T
Research scholar, Professor,
Dept of chemistry,Dept of chemistry,
Central college Central college,
Bengaluru-560001,
Email ID: rajeshwari.gangadhar@gmail.com
Email ID:gtchandrappa@yahoo.co.in

ABSTRACT

In our work, we synthesized dysprosium Zirconium oxide by solution combustion method using dysprosium nitrate, Zirconyl nitrate as an oxidiser and EDTA as a fuel. The synthesized nanopowder was characterized by powder X-ray diffraction (PXRD), scanning electron microscopy (SEM),Breauner Emmet Teller (BET), ultra-violet diffuse reflectance spectrum (UV-DRS) and Photoluminescence (PL) techniques and photo degradation of methylene blue. The PXRD analysis revealed the formation of pure $Dy_{0.5}Zr_{0.5}O_{1.75}$ cubic phase. The crystallite sizes calculated using Scherer's equation is in the range 27.03 nm. SEM images exhibits porous morphology of the synthesized powder. BET surface area analysis of $Dy_{0.5}Zr_{0.5}O_{1.75}$ nano powder shows large specific surface area of 63.22 m^2g^{-1}. Transmission electron microscopy exhibits uniform particle size distribution with average particle sizes varying in the range of 20-100 nm. The band gap of 368.8 nm is calculated using the diffuse reflectance spectrum of $Dy_{0.5}Zr_{0.5}O_{1.75}$. The photoluminescence spectrum of $Dy_{0.5}Zr_{0.5}O_{1.75}$ nanopowder shows emission spectra at 467.2 nm. The photocatalytic activity was carried out by the degradation of methylene blue (MB) using $Dy_{0.5}Zr_{0.5}O_{1.75}$ as photocatalyst showed 80 % of decolourisation in the presence of ultraviolet radiation.

Keywords: Combustion synthesis, Dysprosium Zirconium oxide, Methylene blue and Photocatalytic activity]

I. INTRODUCTION

Zirconium oxide (ZrO_2) is one of the widely studied oxide materials over the last two decades because of its excellent electrical and optical properties, such as high dielectric constant ,good thermal stability, high melting point, and wide band gap (5–7eV) [1, 2]. Zirconium oxide (ZrO_2) is an significant material in the optical fields including broadband interference filters and other active electro- optical devices, due to its outstanding chemical,mechanical and optical properties such as high refractive index, chemical stability, large optical band gap, low optical loss and high transparency in the visible and near infrared region [3, 4]. It shows large band gap and short wavelength Photoluminescence (PL) emission property [5]. Zirconium oxide exhibits different structural polymorphs [6]. The most common ones are monoclinic, tetragonal and cubic phases. The cubic phase (Fm_3m) is a diamond stimulant because of its high refractive index.

Nevertheless, pure ZrO2 is not stable in the cubic phase or tetragonal phase at room temperature. The addition of trivalent dopants like yttrium, gadolinium and dysprosium into ZrO_2 to make stabilize these metastable ZrO_2 phases by creating oxygen vacancies to dynamically favourable such structures. Cubic phase ZrO_2 is mostly stabilized by the addition of up to 20% trivalent rare earth metal oxides. The amount of rare earth in the zirconium oxide also influences on the relevant properties, such as crystal structure and conductivity.

The rare-earth-doped zirconium oxide materials shows distinctive optical properties such as high luminescence efficiency and good chemical stability and photochemical stability [7, 8]. Rare earth doped zirconium oxide have been identified as the most attractive candidates for solid oxide electrolyte in high-temperature fuel cells [9], proton solubility [10], nuclear wastes immobilization [11], and insulation materials

for the outer layer in thermal barrier coatings used in stationary and aircraft gas turbines, and diesel engines [12,13].

In these groups of rare earth doped zirconium oxide, dysprosium doped zirconium oxide is relatively poorly studied [14,15], exclusively in nano range [16]. By doping zirconium oxide, ZrO_2, with dysprosium oxide, Dy_2O_3, a trivalent ion (Zr^{4+}) is substituted by a trivalent one (Dy^{3+}). Due to these properties cubic phases of dysprosium doped ZrO_2 is a stable and should be used in wide and various applications. Therefore synthesis and characterization of nano crystalline dysprosium zirconium oxide has been investigated because of its different properties with respect to the bulk Particles with smaller grain size and higher specific surface .These larger surface area also causes higher catalytic activities and used as a photocatalyst.

Recently, several attempts have been made to prepare Rare earth doped zircons ($RE_2Zr_2O_7$) transparent ceramics. In 2004, transparent $La_2Hf_2O_7$ ceramics with an in-line transmittance above 70% (0.6 mm thick) were successfully fabricated from combustion synthesized powders [17]. Then in 2011, $La_2Zr_2O_7$ transparent ceramics were prepared by reactive spark plasma sintering, [18] but the transmittance was not high enough in the visible region. More recently, Marta Mikuśkiewicz et.al. Synthesized $Dy_2Zr_2O_7$ and investigates its thermal characterization by solid state method [19]. But there is no evidence of reporting the synthesis of $Dy_{0.5}Zr_{0.5}O_{1.75}$ Dysprosium zirconium oxide by combustion method.

The synthesis of Dysprosium zirconium oxide has been achieved by a variety of methods, including solid state reactions and hydrothermal methods. In order to get a material of high quantum efficiency such as better luminescene, good thermal and chemical stability various other synthetic routes have been developed for the synthesis of Dysprosium zirconium oxide such as the co-precipitation, the sol-gel, and solid state method but , high synthesis temperature, long production period, special requirement and low yield are the usual problems of the above method.We thus solved the complexitiesof the above method by establishing a solution combustion method.. High purity nanopowder with a uniform particle size were prepared by solution combustion method (a process of low temperature self-propagating combustion) using EDTA(Ethylenediamine tetra aceticacid) as reaction solvent, dispersant and complexing agent, which could effectively reduce the reaction time, and is currently one of the most promising research directions.

Therefore, the objective of our present work is to synthesize the $Dy_{0.5}Zr_{0.5}O_{1.75}$ (Dysprosium zirconium oxide (non stoichiometric) by combustion reaction using EDTA as fuel and its application in photo degradation of dyes because there is no evidence on reporting the synthesis of $Dy_{0.5}Zr_{0.5}O_{1.75}$ (Dysprosium zirconium oxide) nanopowder by combustion method and its application in photodegradation of dyes.The attempt was made to establish a novel smoldering combustion-type synthesis $Dy_{0.5}Zr_{0.5}O_{1.75}$ (Dysprosium zirconium oxide) nanopowder using a solution of nitrates, with E D TA as the complexing agent and fuel for the reaction. Herein we report the combustion synthesis $Dy_{0.5}Zr_{0.5}O_{1.75}$ (Dysprosium zirconium oxide) because of its high surface area, investigates its photo catalytic property.

II. EXPERIMENTAL SECTION

II.a. Materials required

$Dy(NO_3)_3.6H_2O$, Zirconyl nitrate hydrate and EDTA was purchased from Merck Ltd. and used without further purification.

II.b. Synthesis of $Dy_{0.5}Zr_{0.5}O_{1.75}$ nanopowder

Required amount of aqueous solution of $ZrO(NO_3)_2.6H_2O$ and dysprosium nitrate penta hydrate (Dy:Zr = 1:1) were added to the solution containing Fuel (EDTA). The resultant precursor solution mixture was preheated on a hot plate to get viscous gel which was then placed in a furnace maintained at 500±10 °C Within 10 minute froth was formed undergoing smouldering combustion resulting in the formation of white mass which on calcinations for half an hour yield white coloured highly porous **$Dy_{0.5}Zr_{0.5}O_{1.75}$** (dysprosium Zirconium oxide) nanopowder.

II.c. Photocatalytic degradation

The photocatalytic performance of the as prepared **$Dy_{0.5}Zr_{0.5}O_{1.75}$** nanopowder was evaluated by methylene blue (MB). The photo degradation of MB was carried out in 250 mL pyrex dish in the presence and absence of light. UV light was used as a light source and dark chamber is used as the absence of UV radiation to carry out the experiment. Petridish containing 250 mL MB aqueous solutions (10 ppm) containing as Prepared **$Dy_{0.5}Zr_{0.5}O_{1.75}$** nanopowders (0.1,0.2 and 0.3 g respectively) . The aqueous solution were magnetically stirred in the dark for 30 minutes to establish the adsorption/desorption equilibrium at 25 ^{o}C before illumination. The photocatalytic activity was determined by illuminating the suspensions with UV light. At a given time intervals 5 mL of the sample solution was taken out and separated by centrifugation. The supernatants were analyzed by recording variations in the absorption band maximum (664 nm for MB) using a UV-3101 PC UV-VIS-NIR

scanning spectrophotometer. The photo degradation efficiency of the catalyst was determined by the following expression

$$\text{Dye removal efficiency (\%)} = \frac{C_i - C_f}{C_i} \times 100$$

where, *Ci* and *Cf* are the initial and final dye concentrations

.

III. CHARACTERIZATION

The phase composition of the as prepared powder was analyzed by Powder X-ray diffraction (PXRD) using PANalytical X'pert PRO MPD instrument with graphite-filtered Cu kα radiation source (λ=1.541 Å). Morphology of the $Dy_{0.5}Zr_{0.5}O_{1.75}$ (Dysprosium zirconium oxide) powder was analysed using JEOL-JSM-6490 LV scanning electron microscopy. Nitrogen adsorption–desorption measurements were carried out at 77 K using a gas sorption analyzer (Quantachrome Corporation NOVA 1000) to analyse the textural property. The surface area was calculated using the BET (Breauner emmet teller) method. The band gap of as prepared nano powder were analysed by UV-Visible diffuse reflectance spectrum (UV-VIS DRS) were collected in Uv-Vis range of 200-800 nm with $BaSO_4$ as a reference standard on a shimadzu uv-2450 spectrophotometer at 295 K. The transmission electron microscope were used to analyse the morphology, particle size and composition of each element by energy dispersive X-Ray spectroscopy (EDX). UV-Vis spectrophotometer was used to measure the concentration of dye during degradation process in the max absorbance of 200-800 nm.

IV.RESULTS AND DISCUSSION

IV. a. PXRD (Powder x-ray diffraction)

The PXRD pattern of the $Dy_{0.5}Zr_{0.5}O_{1.75}$ (Dysprosium zirconium oxide) nanopowder prepared by solution combustion process is shown in Figure1. All the Bragg reflections could be indexed to the pure cubic $Dy_{0.5}Zr_{0.5}O_{1.75}$ (Dysprosium zirconium oxide) (JCPDF no.: 78-1293) with lattice parameters a=5.2100. The variation in the broadness of the peaks indicates nano crystalline nature of as synthesized $Dy_{0.5}Zr_{0.5}O_{1.75}$ (Dysprosium zirconium oxide) powder. The crystallite size (D) was estimated based on the line broadening of (*111*) peak at 2θ= 30.02 using the De bye-Scherre'r equation given as $D = K\lambda / \beta \cos\theta$ where λ is the wavelength of the Cu Kα source used, β 1/2 is the full width at half maximum (FWHM) of the (*111*) diffraction peak, K is a shape factor (0.94) and θ is the angle of diffraction which shows the crystallite size as 27.03 nm.

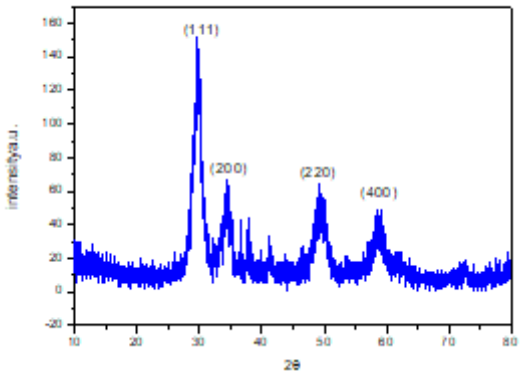

Fig 1 : PXRD Pattern of $Dy_{0.5}Zr_{0.5}O_{1.75}$ (Dysprosium zirconium oxide) nanopowder

IV.b. SEM Analysis (Scanning electron microscopy)

Morphology of the prepared samples were analyzed by using SEM images (Fig.2 a and b) which were taken with the resolution of 10x to 20x respectively. SEM images clearly show porous nature of dysprosium Zirconium oxide nanopowder . The pores and voids created on these layers can be ascribed to the liberation of gas during the reaction.

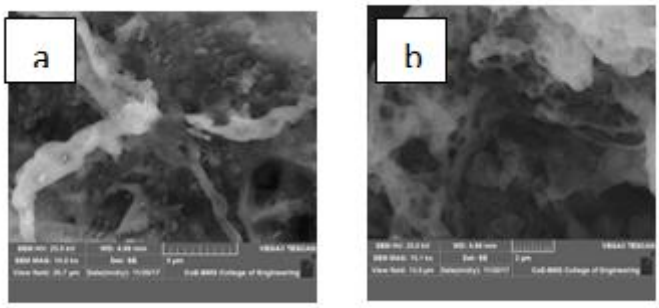

Fig 2 (a and b) : SEM images of Dysprosium Zirconium oxide nanopowder

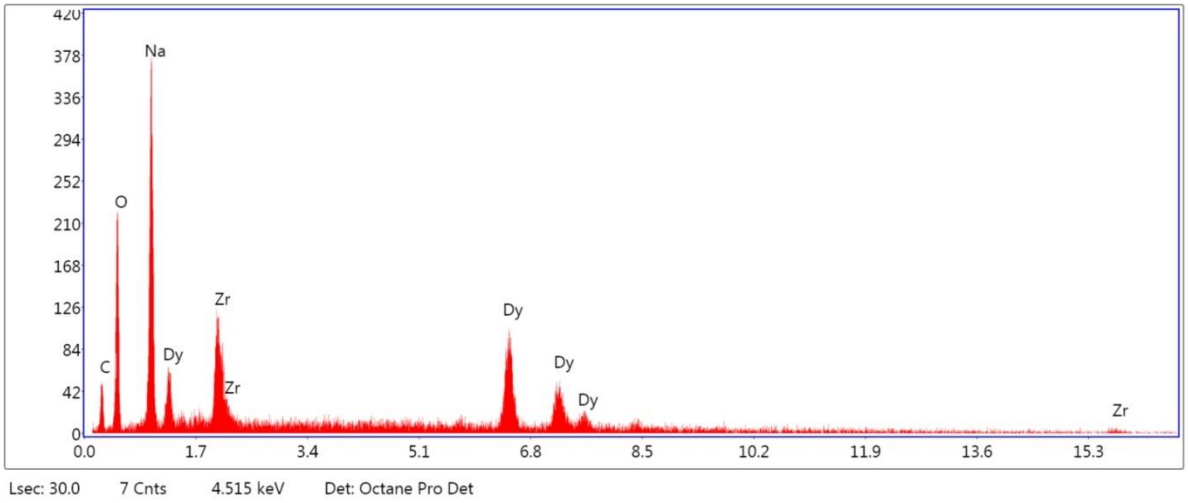

Element	Weight %	Atomic %	Net Int.	Error %	Kratio
C K	16.01	31.33	16.50	16.00	0.0420
O K	28.29	41.55	72.63	12.06	0.0673
NaK	20.37	20.82	137.39	9.56	0.0759
ZrL	10.56	2.72	60.15	12.05	0.0596
DyL	24.76	3.58	91.87	9.16	0.2053

IV.c. BET (Brunauer–Emmett–Teller) surface area

Brunauer–Emmett–Teller (BET) method was used to calculate the specific surface area of the as prepared . $\mathbf{Dy_{0.5}\,Zr_{0.5}\,O_{1.75}}$ nanopowder and is found to be ~63.22 m^2/g. The pore volume was calculated by applying BJH method (Barrett-Joyner-Halenda) for the desorption isotherm data. It showed that 0.085 cc/g total pore volume and 1.556 nm of average pore diameter. Adsorption-desorption isotherm belongs to H_2 type and shows type 2 isotherm. As it is understood, the photo catalytic activity is governed by various factors such as surface area, phase structure, particle size, interfacial charge transfer and separation efficiency of the photo induced electrons and holes. Because if its high surface area it acts as a good photocatalyst.

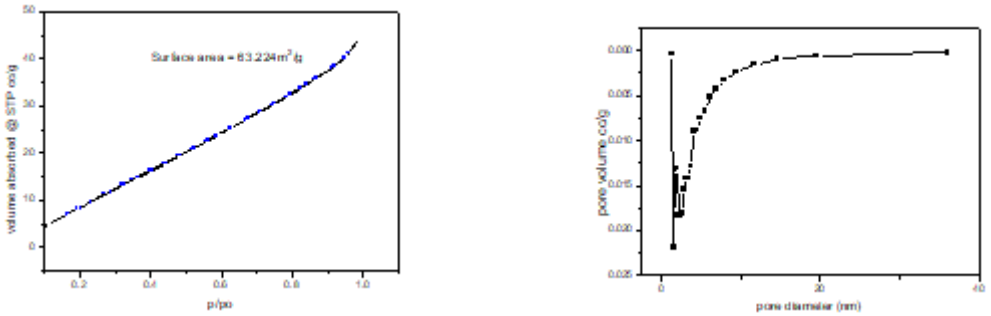

Fig 3(a): Nitrogen adsorption-desorption isotherms and 3(b) corresponding pore-size distribution curves of Dysprosium Zirconium oxide nanopowder

IV.d. UV-Vis absorbance and DRS Studies

The UV-Vis diffuse reflectance spectrum of Dysprosium Zirconium oxide as shown in fig.4 Intercepting the two linearly extrapolated lines ,one can estimate the band gap according to the absorption edge positions.The optical absorbtion edge of dysprosium Zirconium oxide nano powders occurs at 368.8nm, corresponding to bandgap of 3.36 ev calculated using Tauc equation.

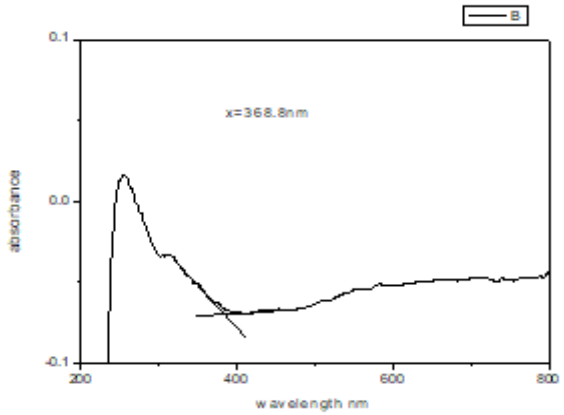

Fig 4: Uv-drs spectrum of Dysprosium Zirconium oxide nanopowder

IV.e. Photoluminescence spectrum

Figure 5 shows the representative PL spectrum of of Dysprosium Zirconium oxide nanopowder with the exited wavelength at 370 nm and corresponding emission peaks centered at 467.4 nm and 504 nm.

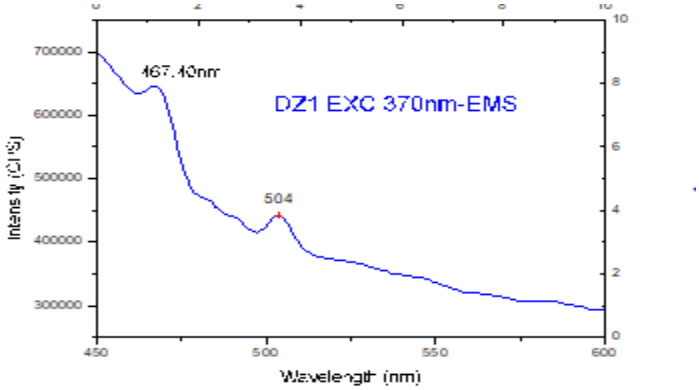

Fig 5: PL spectra of Dysprosium Zirconium oxide nanopowder

IV.f. TEM Analysis (Transmission electron microscopy)

The morphology and structure of Dysprosium Zirconium oxide were further characterized by TEM (Transmission electron microscopy), HRTEM and selected area electron diffraction (SAED) pattern. Figure 6 (a-f) shows the TEM images of the product containing well dispersed irregular shaped agglomerated nanoparticles with average size distribution ranging from 2-100 nm. The SAED pattern (Fig.6g) insisted the typical diffraction pattern of material consists of diffraction rings instead of well defined spots and it shows the crystalline nature of material and lattice spacing 0.30nm corresponds to (111) crystalline plane of cubic phase.

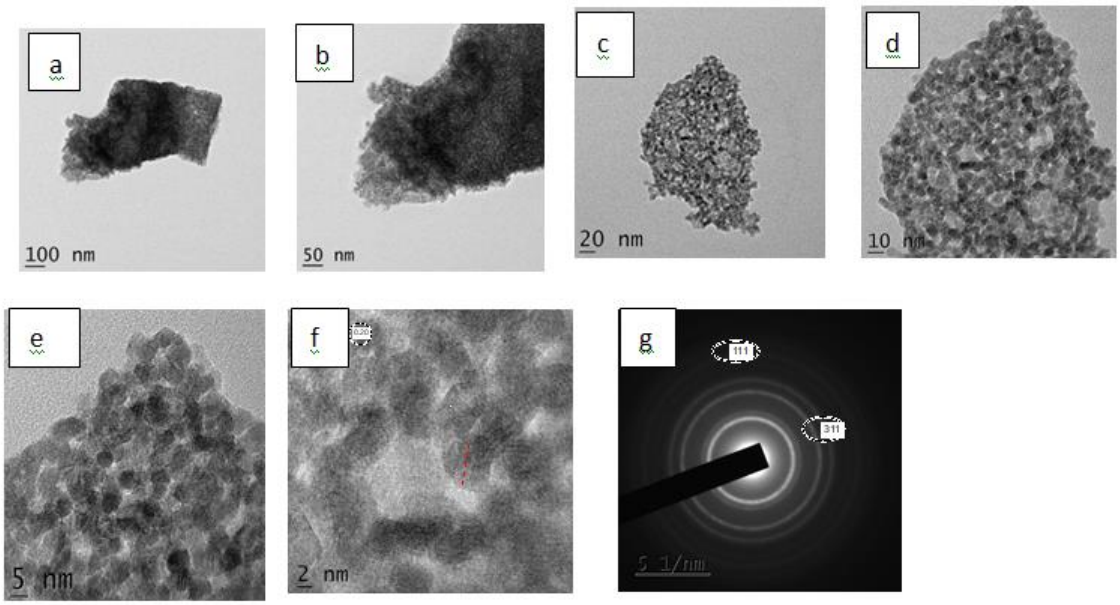

Figure 6(a-f): TEM ,HRTEM images and (g) SAED pattern of dysprosium zirconium powder

IV.f . Phododegradation studies

As it is understood, the photocatalytic activity is governed by various factors such as surface area, phase structure, particle size, interfacial charge transfer and separation efficiency of the photoinduced electrons and holes. Conduction band electrons (e^-) and valance band holes (h^+) are formed when aqueous solution of the photocatalyst of $\mathbf{Dy_{0.5}\ Zr_{0.5}\ O_{1.75}}$ irradiated with light energy greater than the band gap energy of the semiconductor oxide The photogenerated electrons react with absorbed molecular O_2 reducing it to superoxide radical anion O_2^- and photogenerated holes can oxidize organic molecule directly or the H_2O molecule adsorbed at catalyst surface in the presence of ^-OH ions to $^{\cdot}OH$ radical. This $^{\cdot}OH$ radical will act as strong oxidizing agent and can easily attack on organic molecule in the bulk of the solution or those located close to the surface of the catalyst, thus leading to complete mineralization.

Equations shown below represent the probable pathway of the degradation

$$\mathbf{Dy_{0.5}\ Zr_{0.5}\ O_{1.75}} + h\nu \longrightarrow \mathbf{Dy_{0.5}\ Zr_{0.5}\ O_{1.75}} + (h^+ + e^-)$$
$$O_2 + e^- \longrightarrow O_2^{-\cdot}$$
$$R + h \longrightarrow R^+$$
$$h^+ + H_2O \longrightarrow H^+ + {}^{\cdot}OH$$
$$OH + RH \longrightarrow H_2O + R^{\cdot}$$
$$R^{\cdot} + O_2^{\cdot} \longrightarrow ROO^{\cdot} + ROO^{\cdot}$$

Thus decolourization of methylene blue can be investigated in different experimental conditions. 0.3 g of Dysprosium Zirconium oxide was dispersed in 250 mL of 10 ppm MB solution**. Figure 6a** shows the temporal evolution of spectral changes during photocatalytic degradation of 10 ppm MB solution. Separate experiments were carried out to investigate the adsorption activity of the catalyst in dark and self photolysis of MB without catalyst**. Figure 6b** shows the comparison of photo catalytic activity of Dysprosium Zirconium oxide nanopowder with adsorption activity of the catalyst and self photolysis of MB. It is evident that the self

photolysis of MB under uv-irradiation is negligible compared to photo degradation and also it shows that both irradiation and catalyst are necessary for the degradation of dye. **Figure 6c** reveals the comparison of photo catalytic activity of Dysprosium Zirconium oxide nanopowder with different concentration of the catalyst and results that photo catalytic activity is increased from 48% to 80% by increasing the wt of catalysts from 100 to 300 mg due to availability of hydroxyl radicals.The photo degradation efficiency of the catalyst was determined by the following expression:

Dye removal efficiency (%) = $\frac{C_i - C_f}{C_i} \times 100$

where, *Ci* and *Cf* are the initial and final dye concentrations.

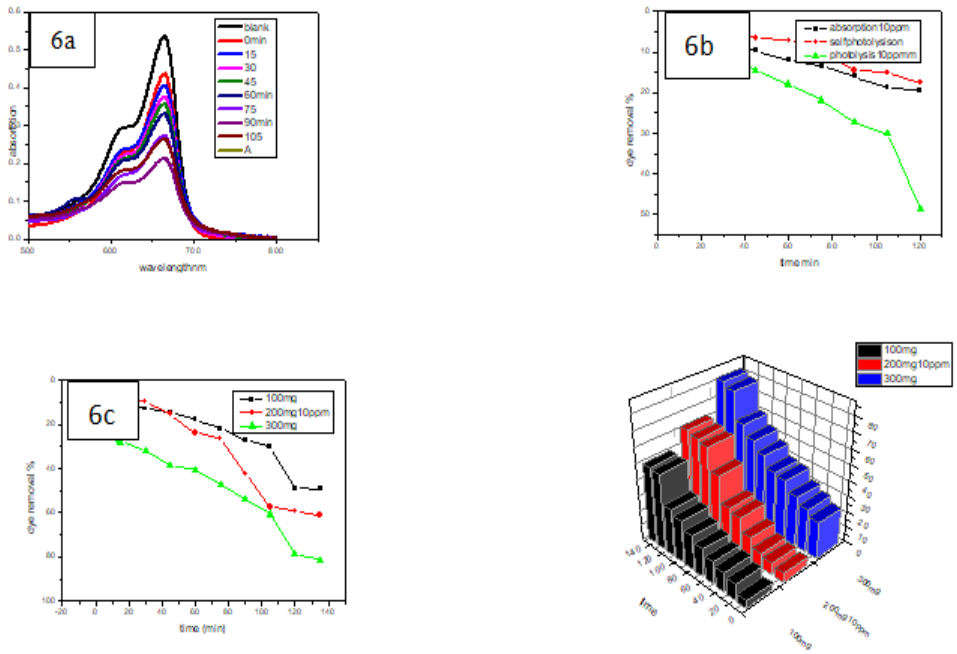

Fig 6 (a) shows the temporal evolution of spectral changes during photodegradation of 10ppm of MB solutionn (b) photo degradation efficiency of dysprosium zirconium oxide nanopowder (c) comparision of photo catalysis with different wt of catalyst.

V. CONCLUSION

In this report, we demonstrate a simple and quick solution combustion synthetic strategy using EDTA as organic fuel to produce highly effective UV light driven $\mathbf{Dy_{0.5}\,Zr_{0.5}\,O_{1.75}}$ photocatalyst. The PXRD pattern shows the formation of cubic phase pure product. The SEM image of $\mathbf{Dy_{0.5}\,Zr_{0.5}\,O_{1.75}}$ nanopowder exhibits porous structure with agglomerated particles. Photocatalytic test revealed good photocatalytic activity of the sample whichcan be attributed to high crystallinity, large surface area and small particle size of the $\mathbf{Dy_{0.5}\,Zr_{0.5}\,O_{1.75}}$ nanopowder.

REFERENCES

[1]. .L. Liao, J. W. Bai, Y. C. Lin, Y. Q. Qu, Y. Huang, and X. F. Duan, Adv. Materials 22,1941 (2010).
[2]. S. J. Wang, and C. K. Ong, Applied Ph+ysics Letters 80, 2541, (2002).
[3]. I. J. Berlin, J. S. Lakshmi, S. S. Lekshmy, G. P. Daniel, P. V. Thomas, and K. Joy, J. gel.Sci. Technol. 58, 669(2011).
[4]. I. John Berlin, L.V. Maneeshya, K. Jijimon, P.V. Thomas, and K. Joy, J. Lumin. 132, 3077 (2012).

[5]. I. John Berlin, V.S. Anitha, P.V. Thomas, and K. Joy, J. Sol–gel Sci. Technol. 64, 289 (2012).
[6]. S. X. Wang, L. M. Wang, and R. C. Ewing, J. Mater. Res., 148, 704–9 (1999).
[7]. Chaudhry A, Canning A, Boutchko R, Weber MJ, Grnbech-Jensen N,Derenzo SE. First-principles studies of Ce-doped $RE_2M_2O_7$ (RE = Y, La; M = Ti, Zr, Hf): a class of non-scintillators. J Appl Phys 2011;109:083708
[8]. T. Ninjbadgar, G.Garnweitner, A.Borger, L. M. Goldenberg, O.V. Sakhno, and J.Stumpe, Advanced Function Materials 19, 1819 (2009).
[9]. H.Hobbs, S.Briddon, and E.Lester, Green Chemistry 11, 484 (2009).
[10]. Labrincha J.A., Frade J.R., Marques F.M.B., Solid State Ionics 99 (1997) 33.
[11]. Takahisa O., Katsuhiko I., Ryoji T., Shinya O.Y.M., Solid State Ionics167 (2004) 389.
[12]. Sickafus K.E., Minervini L., Grimes R.W., Valdez J.A., Ishimaru M., Li F., McClellan K.J.,Hartmann T., Science 289 (2000) 748.
[13]. Moskal G., Swadźba L., Hetmańczyk M., Witala B., Mendala J., Sosnowy P., Journal of The European Ceramic Society 32 (2012) 2025.
[14]. Xu Q., Pan W., Wang J., Qi L., Miao H., Kazutaka M., Taiji T., Materials Letters 59 (2005)2804.
[15]. Cao X., Ma Z., Liu Y., Du Z., Zheng K., Rare Metal Materials and Engineering 42 (2013)1134.
[16]. Popov V. V., Petrunin V. F., Korovin S. A., Menushenkov A. P., Kashurnikova O. V.,Chernikov R. V., Yaroslavtsev A. A., Zubavichus Ya. V., Russian Journal of Inorganic Chemistry 56 (2011) 1538.
[17]. Ji Y, Jiang D, Fen T, Shi J. Fabrication of transparent $La_2Hf_2O_7$ ceramicsfrom combustion synthesized powders. Mater Res Bull 2005;40:553–9.
[18]. An L, Ito A, Goto T. Fabrication of transparent $La_2Zr_2O_7$ by reactive spark plasma sintering. Key Eng Mater 2011;484:135–8.
[19]. Marta Mikuśkiewicz,1,a Michał Stopyra,1,b and Grzegorz Moskal 1,c Synthesis and thermal characterization of dysprosium zirconate Solid State Phenomena Vol. 223 2015) pp 54-61 Submitted: 08.09.201
[20]. G.P.Nagabhushana and G.T. Chandrappa: J.Mater.chem.A,2013,1,11539-11542
[21]. G.P.Nagabhushana,G.Nagaraju and G.T.Chandrappa: J.Mater.chem.A,2013,1,338-394